



Published in final edited form as:

*Biochem Biophys Res Commun.* 2015 July 31; 463(3): 447–452. doi:10.1016/j.bbrc.2015.05.107.

## Identification and characterization of the linear region of ATG3 that interacts with ATG7 in higher eukaryotes

Kazuto Ohashi and Takanori Otomo\*

Department of Integrative Structural and Computational Biology, The Scripps Research Institute, 10550 North Torrey Pines Rd, La Jolla, CA 92037, USA

### Abstract

Transfer of GABARAP thioester from the E1 ATG7 to the E2 ATG3 requires the interaction between the N-terminal domain of ATG7 and the flexible region (FR) of ATG3. This interaction has been visualized in the yeast Atg7-Atg3 complex crystal structure, but remains to be defined in higher eukaryotes. Here, our NMR data precisely define the region of the FR of human ATG3 that interacts with ATG7 (RIA7) and demonstrate RIA7 partially overlaps with the E3-interacting region, explaining how the E1-E2 and E2-E3 interactions are mutually exclusive. Mutational analyses identify critical residues of the RIA7 for the E1 interaction and GABARAP transfer, advancing our understanding of a molecular mechanism of the autophagic conjugation cascade in higher eukaryotes.

### Keywords

autophagy; ubiquitin-like protein; protein-peptide interaction; flexible region; E1-E2 interaction

### Introduction

The members of the autophagy-related protein 8 (Atg8) family of ubiquitin-like proteins are essential for the process of autophagy and include mammalian GABARAP and LC3 and their homologues [1–4]. Atg8 proteins play crucial roles in the expansion and closure of precursor membranes of autophagosomes called phagophores or isolation membranes [2]. Atg8 proteins also contribute to selective autophagy by recruiting cargo to autophagosomes via binding to the tetra-peptide region, the AIM/LIR/LRS motif, of adaptor proteins such as Atg19, Atg32 and p62 [5–7]. All of these activities require conjugation of Atg8 proteins to a lipid molecule, phosphatidylethanolamine (PE), in phagophores [8]. Like ubiquitin and other ubiquitin-like proteins, newly-translated Atg8 undergoes proteolytic cleavage by Atg4 to remove a few residues at its C-terminus, leaving a glycine as the new C-terminal residue of Atg8 [9]. The C-terminal glycine is then adenylated by the E1 enzyme Atg7, followed by conjugation of Atg8 onto the catalytic cysteine residue of Atg7 to form a thioester-bond

\*Correspondence to: Takanori Otomo; totomo@scripps.edu.

**Publisher's Disclaimer:** This is a PDF file of an unedited manuscript that has been accepted for publication. As a service to our customers we are providing this early version of the manuscript. The manuscript will undergo copyediting, typesetting, and review of the resulting proof before it is published in its final citable form. Please note that during the production process errors may be discovered which could affect the content, and all legal disclaimers that apply to the journal pertain.

[10]. Atg8 is then transferred onto the cysteine residue of the E2 enzyme Atg3 via a transthioesterification reaction, followed by transfer of Atg8 to PE by the formation of an isopeptide bond with the aid of the Atg12-Atg5-Atg16 E3 complex [11, 12]. While the chemical reactions involved in this conjugation cascade are essentially the same as those of the canonical ubiquitination cascade [13], the protein-protein interactions involved at each transfer step employ unique structural mechanisms due to the unique domain architectures of the enzymes involved [3]. Atg7 consists of two independently folded domains: a catalytic domain at the C-terminus, which forms a dimer, and an auxiliary domain at the N-terminus. The N- and C-terminal domains are connected to each other via a short linker and the two N-terminal domains (NTD) are located at opposite sides of the C-terminal dimer, forming the wing-like architecture of the full-length dimer [4, 14, 15]. The NTD is unique to Atg7 amongst E1 family proteins and binds to the side of Atg3 opposite its catalytic cysteine residue, poising Atg3 in a position to receive the thioester-linkage between Atg8 and Atg7 (Fig. 1A) [16]. Interestingly, this interface is not sufficient for the overall interaction between Atg3 and Atg7 and the flexible region (FR) of Atg3 located in a middle of its primary sequence supplement the affinity (Fig. 1A) [17]. Accordingly, the FR is required for Atg8-PE conjugation both *in vivo* and *in vitro* [17]. The crystal structure of the *Saccharomyces cerevisiae* Atg3-Atg7 complex showed how the FR interacts with the NTD of Atg7 in the yeast system [16], but this structural information does not appear to apply to higher eukaryotes as the FR sequences are significantly different between yeast and other species [17–19]. While the crystal structure of the *Arabidopsis thaliana* Atg3-Atg7<sup>NTD</sup> complex that shares more sequence homology with the human proteins than yeast is available, the FR is missing from the final model due to the poor electron density for the FR [20] (Fig. 1A). We previously showed that the FR is important for the interaction with E3 in humans and demonstrated that a short region of human ATG3<sup>FR</sup> interacts with ATG12 of E3 (termed the region that interacts with ATG12; RIA12) [18]. On the basis of our structural and biochemical characterizations of this interaction, we proposed that the RIA12 is a novel binding motif for ATG12, another ubiquitin-like protein in autophagy, and is required for recruitment of ATG3 by E3 [18]. Another previous study showed that binding of ATG3 to the E1 and E3 are mutually exclusive due to the overlapping E1 and E3 binding sites within the FR [19]. However, the work was based on protein truncations, leaving the roles of each residue in these binding sites unclear.

To better understand the E1-E2 interaction in higher eukaryotes, we set out to characterize the region of human ATG3 that interacts with ATG7 (RIA7) using biophysical methods and biochemical assays. Nuclear magnetic resonance (NMR) spectroscopy precisely identifies the RIA7 and thus defines the region that is partially overlapping between the RIA7 and the RIA12. Quantitative binding assays using point mutants of ATG3 reveal the importance of each residue in the RIA7 for the E1-E2 interaction and the formation of the GABARAP-E2 thioester conjugate. Mutational analyses on ATG7 confirms the importance of the conserved surface residues of ATG7<sup>NTD</sup>. Collectively, these results establish the residues important for the RIA7-ATG7<sup>NTD</sup> interaction, providing mechanistic insights into the conjugation cascade of autophagic ubiquitin-like proteins.

## Materials and methods

### Preparation of protein materials

Purification of wild-type human ATG3 and mutants were carried out as previously reported [12]. Human ATG7<sup>NTD</sup> was expressed in *E. coli* BL21(DE3) from a modified pET vector with an N-terminal histidine tag and maltose-binding protein tag. Protein expression was induced by addition of 0.2 mM IPTG. After induction, the temperature was reduced to 25°C and the bacteria were harvested after overnight culture.

The proteins were purified using Ni-affinity chromatography, followed by anion-exchange and size-exclusion chromatography. Full-length ATG7 was expressed in Sf9 insect cells using the Bac-to-Bac expression system (Life Technologies) with the pFASTBac vector. The expressed protein was purified using Ni-affinity chromatography followed by anion-exchange and size-exclusion chromatography.

### NMR spectroscopy

NMR experiments were carried out using a Varian Inova 600 MHz spectrometer at 25°C; the protein samples were buffered in 20 mM sodium phosphate pH 6.8, 150 mM NaCl, 2 mM DTT and 10% (v/v) D<sub>2</sub>O. Two <sup>1</sup>H-<sup>15</sup>N HSQC spectra were recorded for 0.3 mM <sup>15</sup>N-labeled ATG3<sup>FR</sup> (residues 88–192) in the absence or presence of 60 μM unlabeled full-length ATG7. The data were processed using NMRPipe and peak intensities were quantified using NMRDraw [21].

### Isothermal titration calorimetry (ITC)

ITC experiments were performed at 25°C using a Microcal VP-ITC. ATG3 proteins (150 μM) were injected into cells filled with 15 μM ATG7<sup>NTD</sup> in 20 mM HEPES pH 7.5, 150 mM NaCl and 1 mM Tris(2-carboxyethyl)phosphine (TCEP) over 25 titrations. The heat generated was quantified and the resulting binding curves were fitted to compute K<sub>d</sub> values and N (stoichiometry) using Origin software (OriginLab).

### GABARAP–ATG3 thioester formation assay

To monitor single turnover thioester formation reactions, 20 μM ATG7 was initially loaded with 10 μM GABARAP in 50 mM HEPES pH 7.0, 150 mM NaCl, 0.3 mM DTT, 200 μM MgCl<sub>2</sub> and 200 μM ATP for 10 min on ice, then the reaction was immediately diluted 10-fold with a solution containing 4 μM ATG3 in 50 mM HEPES pH 7.0, 150 mM NaCl, 0.5 mM DTT and 50 mM EDTA to quench GABARAP loading on ATG7 and initiate the transfer of GABARAP to ATG3. The samples were kept on ice during the experiments and small aliquots were removed from the reaction mixture at the time points indicated in Figure 3. These aliquots were mixed with an equal volume of 2x non-reducing SDS-PAGE sample buffer [100 mM Tris-HCl pH 6.8, 2% (w/v) SDS, 20% (w/v) glycerol and 0.02% (w/v) bromophenol blue] to stop the reaction. The quenched samples were stored on ice until the completion of each time course, then directly loaded onto 12% acrylamide NuPAGE gels (Life Technologies), electrophoresed in MOPS buffer, stained with Coomassie Brilliant Blue G-250 and scanned using an Odyssey infrared imager (Li-cor). The fluorescence intensity of each band was quantified using ImageStudio software (Li-cor).

### GABARAP–PE conjugation assay

GABARAP–PE conjugation reactions were performed as described previously<sup>[12]</sup>. In brief, 1  $\mu\text{M}$  each of ATG7, ATG3 and the ATG12-ATG5-ATG16L1(11–43) complex were mixed with 10  $\mu\text{M}$  GABARAP and liposomes (50  $\mu\text{m}$  diameter; composed of 1 mM total lipids mixed with a molar ratio of 40% DOPC, 40% DOPE and 20% bIPI) in 50 mM HEPES pH 7.5, 150 mM NaCl, 1 mM  $\text{MgCl}_2$  and 0.5 mM DTT. The reactions were initiated at 37°C by adding 1 mM ATP and samples were collected at the indicated time points, mixed with 2x reducing SDS-PAGE buffer and electrophoresed on 13.5% (w/v) acrylamide gels containing 6 M urea. Gel staining, scanning and quantification of GABARAP–PE bands was performed as described above.

### Affinity beads-based binding assay

GST-ATG3 was immobilized on glutathione sepharose 4B resin (GE Healthcare). Beads were washed and resuspended in ATG7 solution so as to contain 2  $\mu\text{M}$  GST-ATG3 and 1  $\mu\text{M}$  ATG7 proteins, 20 mM HEPES pH7.5, 150 mM NaCl, and 0.5 mM TCEP. After incubation for 10 min, the beads were centrifuged at 10,000g for 30 seconds. Supernatants were removed, the beads were washed 3 times and the proteins were eluted in the same buffer containing 30 mM glutathione. The input and elution samples were examined using 12 % NuPage gel as described above.

## Results

### Identification of the RIA7 of human ATG3 by NMR

To precisely identify the RIA7 of human ATG3, we performed two-dimensional  $^1\text{H}$ - $^{15}\text{N}$  heteronuclear single quantum correlation (HSQC) spectroscopic analysis on the isolated ATG3<sup>FR</sup>. Each peak of the spectrum represents a  $^1\text{H}$ - $^{15}\text{N}$  pair in a protein molecule, thus each residue shows at least one peak from the backbone amide bond. As previously shown, all of the peaks in the ATG3<sup>FR</sup> spectrum are intense and distributed within a narrow region of proton chemical shifts, indicating that the ATG3<sup>FR</sup> polypeptide is unfolded [18]. When ATG7 was added to ATG3<sup>FR</sup> at stoichiometric ratio of 0.2, some of the peaks shifted or became broader (Fig. 1B). A change in peak position or intensity is caused by a change in the chemical (electronic) environment close to the atom concerned. The observed peak behaviors suggested that the binding occurs in a so-called intermediate exchange regime where the exchange rate between unbound and bound states is similar to the time scale (ms) of NMR analysis, resulting in a loss of signal intensity. The dissociation constant (Kd) values for such regime are typically in a high  $\mu\text{M}$  range. Thus our observation of intermediate exchange for the ATG3<sup>FR</sup>-ATG7 interaction is consistent with the previously reported Kd value of  $>\sim 70 \mu\text{M}$  [19]. Plotting the residues affected by the addition of ATG7 revealed that the peak intensities in the continuous segment  $\sim 157$ – $181$  of ATG3<sup>FR</sup>, which is located near the terminal carboxyl end, reduced by more than  $\sim 80\%$  (Fig. 1C). This indicates that the residues in the segment  $\sim 157$ – $181$  of ATG3<sup>FR</sup> are involved in ATG7 binding. We previously showed that the segment  $\sim 140$ – $170$  is involved in the interaction with the ATG12–ATG5-ATG16N complex using similar NMR experiments [18]. Thus, the region  $\sim 157$ – $170$  of ATG3<sup>FR</sup> is involved in the interactions with both E1 and E3. This partial

overlapping of the E1 and E3 binding sites explains why the E1-E2 and E2-E3 interactions are mutually exclusive, as previously reported [19].

### **Asp169 of the RIA7 is crucial for the E1-E2 interaction**

Having identified the binding region above, we next sought to uncover the energetic contribution of each of the involved residues to binding. To this end, we quantitatively examined the binding of ATG3 to ATG7<sup>NTD</sup>, the minimal E2 binding unit of ATG7, using isothermal titration calorimetry (ITC). Wild-type ATG3 and ATG7<sup>NTD</sup> bound in a stoichiometric manner with a K<sub>d</sub> value of 0.9 μM (Fig. 2A), which is similar to the value (2.2 μM) reported previously for the interaction between ATG3 and full-length ATG7 [19]. This similarity confirms that most of the binding energy for the E1-E2 interaction is supplied by ATG7<sup>NTD</sup>. We then mutated the conserved residues of the RIA7 of ATG3 and examined the binding of each mutant. Strikingly, single mutation of D169A weakened the ATG3-ATG7<sup>NTD</sup> interaction to such an extent that the data could not be fitted. Mutations of the nearby residues of Asp169, such as E167A, A171G, T172A and L173A, also affected negatively on the binding, with 3 to 4-fold increases in the K<sub>d</sub> values. In contrast, mutations of the residues in the N-terminal region, including those weakened E3 binding (D156A +M157A or Y160A) in our previous study [18], affected modestly, increasing the K<sub>d</sub> values only by 1.6 to 2.9-fold. These results indicate that a rather short C-terminal region within the RIA7 of ATG3 mainly contributes to the binding of ATG7 and the contributions from its N-terminal region, which overlaps with the key region of the RIA12, are markedly less. Next, we examined the ability of these ATG3 mutants to form the thioester-linkage with GABARAP. The results of single turnover assays correlated well with the K<sub>d</sub> values obtained in the ITC analyses; the D169A mutation reduced the transfer of GABARAP severely and the other mutations reduced the transfer to some extent (Fig. 2B). Consistent with the reduced thioester formation, ATG3<sup>D169A</sup> was much less potent than wild-type for the GABARAP-PE conjugation (Fig. 2C). Taken together, these data establish that Asp169 plays the most crucial role in the binding of ATG7 to ATG3 and this interaction is essential for the loading of GABARAP onto ATG3.

### **Conserved surface residues of ATG7<sup>NTD</sup> are crucial for the E1-E2 interaction and GABARAP-loading of ATG3**

In the yeast Atg7-Atg3 complex crystal structure, a part of the FR termed helix C is bound to ScAtg7<sup>NTD</sup> [16]. This binding surface of ScAtg7<sup>NTD</sup> is overall highly basic and consists of the residues conserved among yeast species [14] (Fig. 3A). The same surface location of AtAtg7<sup>NTD</sup> is less conserved and the most highly conserved residues of AtAtg7<sup>NTD</sup>, such as Arg251 and Trp248 (Arg246 and Trp243, respectively, in human ATG7), are located at a position slightly shifted toward the opposite side of the catalytic domain of Atg7 (Fig. 3A and 3B). These residues are located underneath of the poor electron density that was originally suggested to be a part of the FR (Fig. 1A) [20]. We therefore introduced the R246D or W243A mutation in human ATG7 and tested their ability to bind to ATG3 using an affinity-beads-based assay. The result shows that these mutations almost completely or moderately, respectively, impair the ATG3 binding (Fig. 3C). Accordingly, R246D and W243A severely and moderately, respectively, reduced GABARAP-ATG3 thioester bond formation and GABARAP lipidation (Fig. 3D and 3E). Arg246 corresponds to Lys220 of

ScAtg7, which has been shown to be important for the Atg3 binding in the context of simultaneous alanine mutations of three basic residues (K220A+K269A+R275A) (Fig. 3A) [14]. Thus the use of this surface location for the Atg3 binding appears to be evolutionary conserved. However, those three basic residues of ScAtg7 are not in the helix C-binding site and not bound to any other region of the FR of ScAtg3 in the crystal (Fig. 3A)[16]. This is likely because non-specific nature of the electrostatic interaction between those basic residues and acidic residue-rich FR of ScAtg3 results in multiple conformations. In contrast, we have shown that the single residue Arg246, which is in the sole conserved patch of Atg7<sup>NTD</sup>, is crucial for the Atg3 binding and GABARAP transfer. Moreover, there is a short unmodeled density in the crystal structure of the AtAtg3-AtAtg7<sup>NTD</sup>, which must be a part of the FR, as suggested previously, although unambiguous assignment of a peptide region into this unmodeled density may be difficult [20]. Thus we concluded that this conserved patch is the binding surface for the RIA7 and hypothesized that Asp169 of ATG3<sup>RIA7</sup>, the residue important for Atg7 interaction and GABARAP transfer, would form a direct salt bridge with Arg246 of ATG7. We have tested this hypothesis by examining whether a pair of ATG7 and ATG3 in which the charges were swapped, i.e., ATG7<sup>R246D</sup> and ATG3<sup>D169R</sup>, is functional. However, the result was negative in both GABARAP transfer and lipidation assays (data not shown). In the crystal structure of AtAtg7<sup>NTD</sup>, the guanidinium group of Arg251<sup>AtAtg7</sup> is exposed to the solvent and the aliphatic atoms in its side chain makes van der-Waals contacts with other residues including Trp248<sup>AtAtg7</sup>. The Asp-Arg swapping would result in shifting the position of the presumed salt bridge slightly toward the interior of the protein, which may not be favored in such local environment. Further structural study with an aim of visualizing the RIA7 unambiguously would be necessary for clarification of our hypothesis.

## Discussion

As we have shown previously, the N- and C-terminal halves of the RIA12 of human ATG3 have different roles in the ATG12 binding [18]. The N-terminal half, which is highly acidic, contributes to the E3 binding through non-specific electrostatic interactions and the residues in the C-terminal half (residues ~153–165) makes various specific contacts to ATG12 with a  $\mu\text{M}$  range Kd. As shown above, this C-terminal half of the RIA12 overlaps with the N-terminal half of the RIA7 whose contribution to the ATG7 binding is only modest. The key residue ATG3<sup>Asp169</sup> is outside of the RIA12. Thus energetically this overlapping region would favor the E3 over E1 binding, implying that the flow in the E1-E2-E3 reaction cascade is biased toward the downstream PE-conjugation. Consistently, a previous report demonstrated that the ATG12-ATG5-ATG16L1 complex can displace ATG3 from ATG7 but not vice versa [19]. This raises a question regarding how the shuttling of ATG3 between of the E1 and E3, which is necessary for multiple turnover of this process, would be achieved. Thorough kinetic and thermodynamic studies will be required for understanding the dynamic nature of this important E1-E2-E3 cascade in autophagy.

## Supplementary Material

Refer to Web version on PubMed Central for supplementary material.

## Acknowledgements

This work was supported by a National Institute of Health (NIH) grant GM092740 to T.O. and a JSPS (Japanese Society for the Promotion of Science) post-doctoral fellowship award to K.O.

## Abbreviations

<b>Atg/ATG</b>	Autophagy-related
<b>NMR</b>	nuclear magnetic resonance
<b>HSQC</b>	heteronuclear single quantum correlation
<b>ITC</b>	isothermal titration calorimetry
<b>RIA12</b>	region that interacts with ATG12
<b>RIA7</b>	region that interacts with ATG7
<b>FR</b>	flexible region
<b>NTD</b>	amino-terminal domain
<b>PE</b>	phosphatidylethanolamine

## References

- [1]. Geng J, Klionsky DJ. The Atg8 and Atg12 ubiquitin-like conjugation systems in macroautophagy. 'Protein modifications: beyond the usual suspects' review series, *EMBO Rep.* 2008; 9:859–864. [PubMed: 18704115]
- [2]. Mizushima N, Yoshimori T, Ohsumi Y. The role of Atg proteins in autophagosome formation. *Annu Rev Cell Dev Biol.* 2011; 27:107–132. [PubMed: 21801009]
- [3]. Hurley JH, Schulman BA. Atomistic autophagy: the structures of cellular self-digestion. *Cell.* 2014; 157:300–311. [PubMed: 24725401]
- [4]. Klionsky DJ, Schulman BA. Dynamic regulation of macroautophagy by distinctive ubiquitin-like proteins. *Nat Struct Mol Biol.* 2014; 21:336–345. [PubMed: 24699082]
- [5]. Pankiv S, Clausen TH, Lamark T, Brech A, Bruun JA, Outzen H, Overvatn A, Bjorkoy G, Johansen T. p62/SQSTM1 binds directly to Atg8/LC3 to facilitate degradation of ubiquitinated protein aggregates by autophagy. *J Biol Chem.* 2007; 282:24131–24145. [PubMed: 17580304]
- [6]. Ichimura Y, Kumanomidou T, Sou YS, Mizushima T, Ezaki J, Ueno T, Kominami E, Yamane T, Tanaka K, Komatsu M. Structural basis for sorting mechanism of p62 in selective autophagy. *J Biol Chem.* 2008; 283:22847–22857. [PubMed: 18524774]
- [7]. Noda NN, Ohsumi Y, Inagaki F. Atg8-family interacting motif crucial for selective autophagy. *FEBS Lett.* 2010; 584:1379–1385. [PubMed: 20083108]
- [8]. Ichimura Y, Kirisako T, Takao T, Satomi Y, Shimonishi Y, Ishihara N, Mizushima N, Tanida I, Kominami E, Ohsumi M, Noda T, Ohsumi Y. A ubiquitin-like system mediates protein lipidation. *Nature.* 2000; 408:488–492. [PubMed: 11100732]
- [9]. Kirisako T, Ichimura Y, Okada H, Kabeya Y, Mizushima N, Yoshimori T, Ohsumi M, Takao T, Noda T, Ohsumi Y. The reversible modification regulates the membrane-binding state of Apg8/Aut7 essential for autophagy and the cytoplasm to vacuole targeting pathway. *The Journal of cell biology.* 2000; 151:263–276. [PubMed: 11038174]
- [10]. Mizushima N, Noda T, Yoshimori T, Tanaka Y, Ishii T, George MD, Klionsky DJ, Ohsumi M, Ohsumi Y. A protein conjugation system essential for autophagy. *Nature.* 1998; 395:395–398. [PubMed: 9759731]

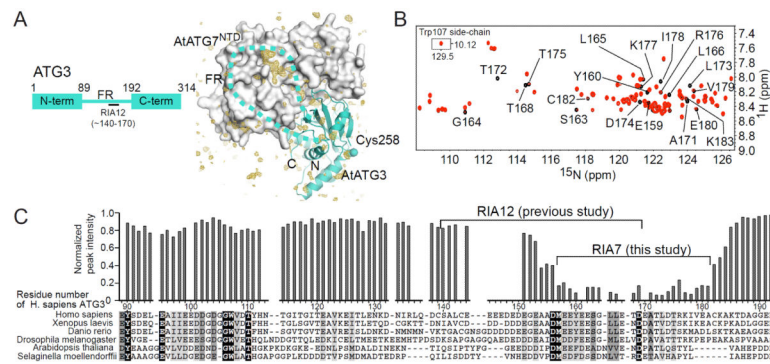
- [11]. Hanada T, Noda NN, Satomi Y, Ichimura Y, Fujioka Y, Takao T, Inagaki F, Ohsumi Y. The Atg12-Atg5 conjugate has a novel E3-like activity for protein lipidation in autophagy. *J Biol Chem.* 2007; 282:37298–37302. [PubMed: 17986448]
- [12]. Otomo C, Metlagel Z, Takaesu G, Otomo T. Structure of the human ATG12~ATG5 conjugate required for LC3 lipidation in autophagy. *Nat Struct Mol Biol.* 2013; 20:59–66. [PubMed: 23202584]
- [13]. Schulman BA, Harper JW. Ubiquitin-like protein activation by E1 enzymes: the apex for downstream signalling pathways. *Nat Rev Mol Cell Biol.* 2009; 10:319–331. [PubMed: 19352404]
- [14]. Noda NN, Satoo K, Fujioka Y, Kumeta H, Ogura K, Nakatogawa H, Ohsumi Y, Inagaki F. Structural basis of Atg8 activation by a homodimeric E1, Atg7. *Mol Cell.* 2011; 44:462–475. [PubMed: 22055191]
- [15]. Taherbhoy AM, Tait SW, Kaiser SE, Williams AH, Deng A, Nourse A, Hammel M, Kurinov I, Rock CO, Green DR, Schulman BA. Atg8 transfer from Atg7 to Atg3: a distinctive E1-E2 architecture and mechanism in the autophagy pathway. *Mol Cell.* 2011; 44:451–461. [PubMed: 22055190]
- [16]. Kaiser SE, Mao K, Taherbhoy AM, Yu S, Olszewski JL, Duda DM, Kurinov I, Deng A, Fenn TD, Klionsky DJ, Schulman BA. Noncanonical E2 recruitment by the autophagy E1 revealed by Atg7-Atg3 and Atg7-Atg10 structures. *Nat Struct Mol Biol.* 2012; 19:1242–1249. [PubMed: 23142976]
- [17]. Yamada Y, Suzuki NN, Hanada T, chimura Y, Kumeta H, Fujioka Y, Ohsumi Y, Inagaki F. The crystal structure of Atg3, an autophagy-related ubiquitin carrier protein (E2) enzyme that mediates Atg8 lipidation. *J Biol Chem.* 2007; 282:8036–8043. [PubMed: 17227760]
- [18]. Metlagel Z, Otomo C, Takaesu G, Otomo T. Structural basis of ATG3 recognition by the autophagic ubiquitin-like protein ATG12. *Proc Natl Acad Sci U S A.* 2013; 110:18844–18849. [PubMed: 24191030]
- [19]. Qiu Y, Hofmann K, Coats JE, Schulman BA, Kaiser SE. Binding to E1 and E3 is mutually exclusive for the human autophagy E2 Atg3. *Protein Sci.* 2013; 22:1691–1697. [PubMed: 24186333]
- [20]. Yamaguchi M, Matoba K, Sawada R, Fujioka Y, Nakatogawa H, Yamamoto H, Kobashigawa Y, Hoshida H, Akada R, Ohsumi Y, Noda NN, Inagaki F. Noncanonical recognition and UBL loading of distinct E2s by autophagy-essential Atg7. *Nat Struct Mol Biol.* 2012; 19:1250–1256. [PubMed: 23142983]
- [21]. Delaglio F, Grzesiek S, Vuister GW, Zhu G, Pfeifer J, Bax A. NMRPipe: a multidimensional spectral processing system based on UNIX pipes. *J Biomol NMR.* 1995; 6:277–293. [PubMed: 8520220]
- [22]. Glaser F, Pupko T, Paz I, Bell RE, Bechor-Shental D, Martz E, Ben-Tal N. ConSurf: identification of functional regions in proteins by surface-mapping of phylogenetic information. *Bioinformatics.* 2003; 19:163–164. [PubMed: 12499312]

### Highlights

The region of human ATG3 that interacts with ATG7 is precisely identified using NMR.

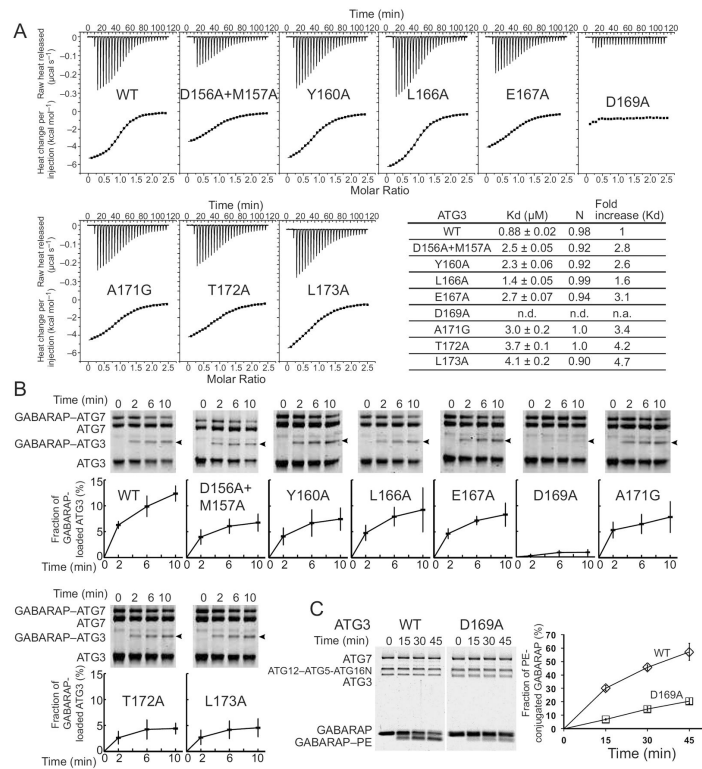
Biochemical and interaction assays identify Asp169 of human ATG3 as the key residue for ATG7-ATG3 interaction.

Biochemical analyses confirm the importance of the conserved small patch of ATG7 in ATG3 binding.

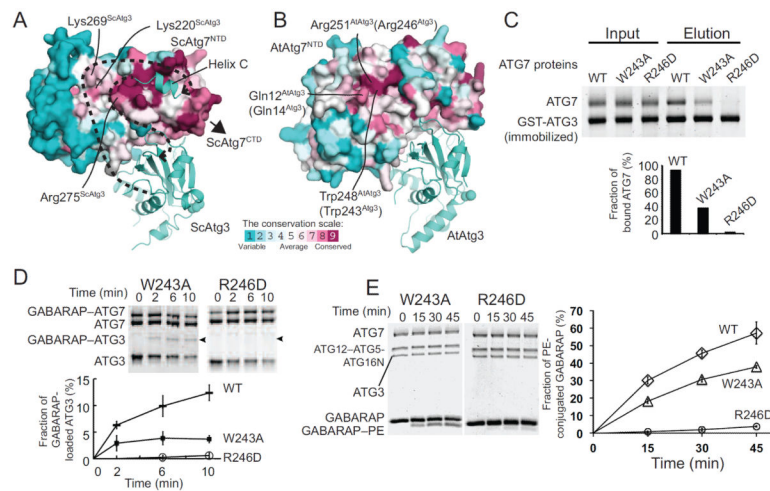


**Figure 1.**

NMR analyses of the ATG3<sup>FR</sup>-ATG7 interaction. (A) Schematic illustration of the human ATG3 polypeptide chain (right) and the crystal structure of AtAtg3 (cartoon model) bound to AtAtg7<sup>NTD</sup> (gray surface; PDB entry 3vx8). The mFo-DFc difference map contoured at 3σ is also shown to indicate the unmodeled density [20]. (B) Overlay of <sup>1</sup>H-<sup>15</sup>N HSQC spectra for human ATG3<sup>FR</sup> (residues 92–192) recorded in the absence (black) or presence (red) of ATG7. (C) Normalized peak intensity ratios in the presence and absence of ATG7 are plotted against the sequence of ATG3 aligned with other species, as indicated. The positions with a ratio of zero are those missing an assigned peak. Residues that are completely conserved or change to a similar type of amino acid are shaded with black and gray, respectively.

**Figure 2.**

Effects of mutations in ATG3<sup>RIA7</sup>. (A) Quantification of the contributions of the conserved residues of ATG3<sup>RIA7</sup> to the interaction with ATG7<sup>NTD</sup> using ITC. ATG3 proteins were injected into ATG7<sup>NTD</sup> (15 $\mu\text{M}$ ) solution. Kd values and N (stoichiometry) obtained by fitting the titration curves to the single-binding isotherm are indicated in the right bottom table. (B) Single turnover GABARAP–ATG3 thioester formation assays and (C) GABARAP–PE conjugation assays for ATG3 mutants. For each mutant, a representative result of SDS-PAGE for a time course of GABARAP–ATG3 thioester formation (B) or the GABARAP–PE conjugation (C) are shown with quantification. The arrows in (B) indicate GABARAP–ATG3 thioester conjugates for clarity. Each data point represents the mean  $\pm$  the standard deviations of three independent experiments.

**Figure 3.**

Confirmation of the ATG3-binding site on ATG7<sup>NTD</sup>. (A) The crystal structure of ScAtg3-ScAtg7 complex (PDB entry 4gsl). Cartoon and surface models, respectively, of AtAtg3 and the AtAtg7<sup>NTD</sup> are shown. ScAtg7<sup>CTD</sup> (catalytic domain) is omitted but its position relative to ScAtg7<sup>NTD</sup> is indicated by an arrow. Each residue of ScAtg7 was given a conservation score calculated on ConSurf server [22] using a sequence alignment of Atg7 from yeast species and is colored as indicated. (B) The crystal structure of the AtAtg3-AtAtg7<sup>NTD</sup> complex (PDB entry 3vx8) is shown in a similar manner as in (A). The conservation scores were obtained using sequences of Atg7 from eukaryotic species excluding yeast. (C) Binding of ATG7 mutants to an immobilized GST-ATG3. An SDS-PAGE of the inputs and elution solutions and the fractions of the amounts of ATG7 proteins in the elution solutions over those in the inputs are shown. (D) Single turnover GABARAP-ATG3 thioester formation assays and (E) GABARAP-PE conjugation assays for ATG7 mutants. The data in (D) and (E) are presented in the same manner as in Figures 2B and 2C, respectively. The controls with wild-type ATG7 in (D) and (E) are shown in Figures 2B and 2C, respectively, as wild-type ATG3.